

# Initiation of shape instabilities of free boundaries in planar Cauchy–Stefan problems

QIANG ZHU, ANTHONY PEIRCE and JOHN CHADAM

*Department of Mathematics and Statistics, McMaster University, Hamilton, Ontario L8S 4K1, Canada*

*(Received 8 April 1992)*

The linearized shape stability of melting and solidifying fronts with surface tension is discussed in this paper by using asymptotic analysis. We show that the melting problem is always linearly stable regardless of the presence of surface tension, and that the solidification problem is linearly unstable without surface tension, but with surface tension it is linearly stable for those modes whose wave numbers lie outside a certain finite interval determined by the parameters of the problem. We also show that if the perturbed initial data is zero in the vicinity of the front, but otherwise quite general, it does not affect the stability. The present results complement those in Chadam & Ortoleva [4] which are only valid asymptotically for large time or equivalently for slow-moving interfaces. The theoretical results are verified numerically.

## 1 Introduction

There has been considerable interest in the shape instabilities of moving free boundary problems which arise as models of physically important phenomena. In this note we study the criteria for the onset of instabilities of a planar solidification solution of the 1-phase Stefan problem with surface tension (see equations (1)–(5) in §2). This may be considered as a simplified mathematical model of the solidification of a pure alloy neglecting temperature effects (see Mullins & Sekerka [1] and Langer [2] for a discussion of this class of models). Morphological instabilities of this sort are generally called Mullins–Sekerka instabilities after their initial study [1] of a quasi-stationary version (diffusion equation replaced by Laplace’s equation which is compatible with slow-moving fronts) of the present model. The stability of melting fronts has been treated by Turland & Peckover [3] in the context of a 2-phase version of this model. Chadam & Ortoleva [4] obtained results for the present model in qualitative agreement with those obtained for the quasi-stationary version (see [2] for a recent summary) for slow-moving solidification fronts and with Turland & Peckover’s 2-phase version for melting fronts. In the present work we generalize those of Chadam & Ortoleva [4] to solidification fronts moving with arbitrary velocity.

This work, as does [4], studies the stability of shape perturbations of  $x/2\sqrt{t}$  similarity planar solutions with the front positioned at  $\alpha\sqrt{t}$ . It has been shown in [5], and by Ricci & Xie [6] with a more complete analysis, that the above similarity solution is the global attractor of all planar solutions with the same Stefan number ( $ku_\infty$  in the notation of equations (1)–(5) in §2), if  $ku_\infty < 1$ . That is, if  $ku_\infty < 1$ , any planar solution with the interface initially at  $R(0)$ , arbitrary, and with sufficiently regular data  $(u_\infty - u_0(x))$  and  $x(u_\infty - u_0(x))$  belonging to  $L^1(R(0), \infty)$  evolves with its interface always within a finite

distance of the  $\alpha \sqrt{t}$  interface of the similarity solution selected by the desiderata  $ku_\infty$  [5, 6]. It is for this reason that we use the  $x/2 \sqrt{t}$  similarity solutions as the base planar solutions about which the linearized stability is performed. It should be noted that for  $ku_\infty > 1$  these similarity solutions are not available, and indeed, the model in equations (1)–(5) of §2 breaks down in that it admits planar solutions for which the velocity of the front blows up in finite time [5]. Travelling wave solutions to this problem are only available at the critical value  $ku_\infty = 1$  (corresponding to  $\alpha = \infty$  in the similarity solution) with the velocity depending on the rate at which the initial data approaches  $u_\infty$  [6, 8]. As such, these travelling wave solutions are inappropriate as the planar solutions on which to base the stability analysis. On the other hand, the use of the time-dependent similarity solutions leads to more complicated differential equations for the amplitudes of the perturbations in that they have variable coefficients. As a result, the analysis must be carried out at some fixed time  $T$  with the front at the position  $\alpha \sqrt{T}$ . As one might expect, the stability criterion which is derived in this paper does not depend on the position of the front but rather has the  $T$  dependence enter through the velocity of the front,  $V = \alpha/2 \sqrt{T}$ . This work generalizes that in [4], which required that  $T \rightarrow \infty$ , or equivalently, if  $R = \alpha \sqrt{T}$  is to remain finite, that  $\alpha$  and hence  $V = \alpha/2 \sqrt{T} \rightarrow 0$ .

For time-dependent stability problems of this sort, it has been observed [7] that the growth of a perturbation at a particular time can depend quite dramatically on the initial behaviour of the concentration field in the vicinity of the front. In this study we are specifically attempting to preclude this situation by considering instabilities that are autonomously selected by geometric interactions. We therefore restrict our study to the situation in which the planar front is evolving with the concentration field having reached the planar equilibrium value in the vicinity of the front. Analytically, we impose a strong version of this condition, demanding that the perturbed concentration field be identically zero in some interval ahead of the front. We show that for perturbations of this sort which, away from the front, can be quite general, the instability is determined by the autonomous geometric selection of instabilities and not the particular form of the initial concentration perturbation.

In §2 we introduce the model problem and derive a boundary integral equation for the amplitude function governing the linearized shape stability, which involves a complicated double integral. We then derive a set of coupled integral and integro-differential equations which are equivalent to the former but which only involve single integrals. In §3 we derive the asymptotic estimates of the solutions of the integral equations. These estimates are then used to derive the asymptotic behaviour of the amplitude of the shape perturbations in §4. Physical interpretation of these theoretical results are also given in §4. The results of §3 and 4 are computationally intensive, and are presented in theorem-proof form for precision and to facilitate the flow of rather long arguments. The proofs are not rigorous (i.e. errors are not controlled), but serve to indicate the location of the arguments. The numerical verification of the results is outlined in §5. A summary is given in §6.

## 2 Model problem and integral equation formulation

The simplified non-dimensional form of the model [4] is

$$\frac{\partial u}{\partial t} = \Delta u, \quad Q(x, t) > 0, t > T, \quad (1)$$

$$u = \gamma K, \quad \text{on } Q(x, t) = 0, t > T, \quad (2)$$

$$\nabla u \cdot \nabla Q = -k^{-1} Q, \quad \text{on } Q(x, t) = 0, t > T, \quad (3)$$

$$u(x, T) = u_0(x), \quad \text{in } Q(x, T) = Q_0(x) > 0, \quad (4)$$

$$u(x, t) \rightarrow u_\infty, \quad \text{as } |x| \rightarrow \infty, t \geq T, \quad (5)$$

where  $u$  is the concentration of the melt,  $Q(x, t) = 0$  is the solid-melt interface with the solid occupying  $Q(x, t) < 0$ ,  $K = (2|\nabla Q|^3)^{-1} [|\nabla Q|^2 \Delta Q - \frac{1}{2} \nabla(|\nabla Q|^2) \nabla Q]$  is the mean curvature of the interface, and  $k > 0$  is a constant. The equilibrium concentration in (2) has been taken to be zero by a change of variable. In addition,  $T > 0$  is the initial time,  $x \in R^3$ ,  $t \in [T, \infty)$ ,  $\gamma \geq 0$  and  $u_\infty$ , the ambient concentration, are constants. When  $\gamma = 0$ , problem (1)–(5) is a standard Stefan problem. With  $\gamma \neq 0$  a higher concentration – the Gibbs–Thomson relation – is required on the boundary to maintain a more curved configuration.

While there is always a difficulty with mass loss in one-phase problems with surface tension and constant  $k$ , the above model problem might be considered a reasonable approximation in the almost-planar context of current interest. A more general version for which mass is conserved has  $k^{-1}$  in equation (3) replaced by  $\rho - u$  (interface), where  $\rho$  is the density of the solid and the concentration at the interface,  $u$  (interface) =  $\gamma K$  from equation (2) [1]. Since at the onset of instability the interface is almost planar (i.e.  $K$  small) so that  $\rho \gg \gamma K$  and hence  $k^{-1} = (\rho - \gamma K) \simeq \rho$  a constant. In addition, since we are interested in solidification fronts with arbitrary velocities, the diffusion equation is used for the concentration field in equation (1) rather than the quasi-stationary version [1] using the Laplace equation. This latter is only compatible with fronts moving very slowly so that the external concentration field can be maintained at steady-state.

With  $Q(x, t) = x - R(t)$  the planar version of problem (1)–(5) is

$$\frac{\partial u}{\partial t} = \frac{\partial^2 u}{\partial x^2}, \quad x > R(t), t > T, \quad (6)$$

$$u = 0, \quad \text{on } x = R(t), t > T, \quad (7)$$

$$\frac{\partial u}{\partial x} = k^{-1} \dot{R}(t), \quad \text{on } x = R(t), t > T, \quad (8)$$

$$u(x, T) = u_0(x), \quad x > R(T), \quad (9)$$

$$u(x, t) \rightarrow u_\infty, \quad \text{as } x \rightarrow +\infty, t \geq T. \quad (10)$$

Clapeyron & Lamé [9] found a similarity solution of (6)–(10)

$$u_p(x, t) = -(\alpha/k) e^{x^2/4} \int_{x/2\sqrt{t}}^{\infty} e^{-y^2} dy + u_\infty, \quad (11)$$

$$R_p(t) = \alpha \sqrt{t} \quad (12)$$

where  $\alpha$  satisfies the equation

$$\alpha e^{\alpha^2/4} \int_{\alpha/2}^{\infty} e^{-y^2} dy = k u_{\infty}. \quad (13)$$

Clearly, the signs of  $\alpha$  and  $u_{\infty}$  are the same. Here  $\alpha < 0$  corresponds to the melting problem, and  $\alpha > 0$  corresponds to the solidification problem. We assume that  $\alpha \neq 0$  in this paper.

It has been shown that the similarity solution is asymptotically stable in the class of planar solutions in [5], and with a more complete analysis in [6]. More precisely, with some technical conditions on the initial data  $u_0(x)$ , the difference between the similarity solution (11)–(13) and any planar solution with the same  $k, u_{\infty}$  is finite for all time. Thus, studying the shape stability of any planar solution reduces to studying the shape stability of the corresponding similarity solution (11)–(13). As mentioned above, the asymptotic shape stability ( $T, t \rightarrow \infty$ ) has already been studied in [4]. This corresponds to slow-moving fronts, since if the initiation position  $R_p(T) = \alpha \sqrt{T}$  is to remain finite, then  $\alpha$  and hence the velocity of the front  $V = \dot{R}_p(T) = \alpha/2 \sqrt{T}$  must tend to zero. Here we will discuss the shape stability for arbitrary, finite, initial time  $T$ . This represents an essential difference from the results of [4] in that it provides information about the initiation of instabilities at finite times with finite velocities.

Considering non-planar perturbations, we write

$$u_{\epsilon}(x, y, t) = u_p(x, t) + \epsilon u(x, y, t) + O(\epsilon^2), \quad (14)$$

$$x = R_{\epsilon}(y, t) = R_p(t) + \epsilon R(y, t) + O(\epsilon^2). \quad (15)$$

Substituting (14) and (15) into (1)–(5), we obtain the following equations for the perturbations  $u(x, y, t)$  and  $R(y, t)$

$$\frac{\partial u}{\partial t} = \Delta u, \quad x > R_p(t), t > T, \quad (16)$$

$$u = -\frac{\partial u_p}{\partial x} R - \frac{\gamma}{2} \frac{\partial^2 R}{\partial y^2}, \quad \text{on } x = R_p(t), t > T, \quad (17)$$

$$\frac{\partial u}{\partial x} = k^{-1} \frac{\partial R}{\partial t} - \frac{\partial^2 u_p}{\partial x^2} R, \quad \text{on } x = R_p(t), t > T, \quad (18)$$

$$u(x, y, T) = \Phi(x, y), \quad x > R_p(T), \quad (19)$$

$$u(x, y, t) \rightarrow 0, \quad \text{as } x \rightarrow \infty, t \geq T. \quad (20)$$

Making the change of variables

$$q = u + \frac{\partial u_p}{\partial x} R + \frac{\gamma}{2} R_{yy} \quad (21)$$

and letting

$$q(x, y, t) = w(x, t) e^{-t^2} e^{u_p}, \quad (22)$$

$$R(y, t) = f(t) e^{u_p}, \quad (23)$$

( $|l| > 0$ ), we obtain

$$\frac{\partial w}{\partial t} - \frac{\partial^2 w}{\partial x^2} + [f(t) + l^2 f(t)] \left( -\frac{\partial u_p}{\partial x} + \frac{\gamma l^2}{2} \right) e^{l^2 t} = 0, \quad x > R_p, t > T, \tag{24}$$

$$w = 0, \quad \text{on } x = R_p(t), t > T, \tag{25}$$

$$\frac{\partial w}{\partial x} = k^{-1} f(t) e^{l^2 t}, \quad \text{on } x = R_p(t), t > T, \tag{26}$$

$$w(x, T) = \chi(x), \quad x > R_p(T), \tag{27}$$

$$w(x, t) \rightarrow -\frac{\gamma l^2}{2} f(t) e^{l^2 t}, \quad \text{as } x \rightarrow +\infty, t \geq T. \tag{28}$$

If  $E(x, \xi, t, \tau) = 1/(2 \sqrt{[\pi(t-\tau)]}) e^{[-(x-\xi)^2/4(t-\tau)]}$  denotes the fundamental solution of the heat equation, using the divergence theorem and taking into account the double layer discontinuity of the heat potential, we obtain:

$$\begin{aligned} \frac{\partial w}{\partial x}[R_p(t), t] &= 2 \int_{R_p(\tau)}^{\infty} \chi(\xi) E_x[R_p(t), \xi, t, T] d\xi + 2 \int_{\tau}^t d\tau \int_{R_p(\tau)}^{\infty} d\xi \left\{ \left[ \frac{\partial u_p}{\partial x}(\xi, \tau) - \frac{\gamma l^2}{2} \right] \right. \\ &\quad \left. \times [f(\tau) + l^2 f(\tau)] e^{l^2 \tau} E_x[R_p(t), \xi, t, \tau] \right\} - 2 \int_{\tau}^t \frac{\partial w}{\partial x}[R_p(\tau), \tau] E_x[R_p(t), R_p(\tau), t, \tau] d\tau. \end{aligned} \tag{29}$$

Following Rubinstein [10] and Chadam & Ortoleva [4], this equation can be decoupled into the following integro-differential equation

$$\dot{f}(t) = kI(t) e^{-l^2 t} + k \int_{\tau}^t [f(\tau) + l^2 f(\tau)] e^{-l^2(t-\tau)} \times [P(t, \tau) + \Gamma(t, \tau)] d\tau, \tag{30}$$

where the kernels  $P, \Gamma$  and the inhomogenous term  $I$  are found to satisfy

$$P(t, \tau) = 2 \int_{R_p(\tau)}^{\infty} \frac{\partial u_p}{\partial x}(\xi, \tau) E_x[R_p(t), \xi, t, \tau] d\xi - 2 \int_{\tau}^t P(\mu, \tau) E_x[R_p(t), R_p(\mu), t, \mu] d\mu, \tag{31}$$

$$\Gamma(t, \tau) = -\gamma l^2 \int_{R_p(\tau)}^{\infty} E_x[R_p(t), \xi, t, \tau] d\xi - 2 \int_{\tau}^t \Gamma(\mu, \tau) E_x[R_p(t), R_p(\mu), t, \mu] d\mu, \tag{32}$$

$$I(t) = 2 \int_{R_p(\tau)}^{\infty} \chi(\xi) E_x[R_p(t), \xi, t, T] d\xi - 2 \int_{\tau}^t I(\tau) E_x[R_p(t), R_p(\tau), t, \tau] d\tau. \tag{33}$$

Examining the linearized shape stability is equivalent to discussing the asymptotic behaviour of the amplitude  $f(t)$  as  $t - T \rightarrow 0^+$ . In [4], the asymptotic behaviour of  $f(t)$  was examined for  $T, t \rightarrow +\infty$ . It was pointed out that the results agreed with those derived by Ockendon [11] using different methods but left open the possibility that other instabilities might occur at short times. The present analysis generalizes that of [4, 11], and agrees with it when  $T \rightarrow \infty$  (equivalently  $\alpha \rightarrow 0$ ).

### 3 Asymptotic estimates of $P(t, \tau), \Gamma(t, \tau)$ and $I(t)$

From (30) we have  $T \leq \tau \leq t$ , so  $t - \tau \rightarrow 0^+$  if  $t - T \rightarrow 0^+$ . If we find the asymptotic behaviour of  $P(t, \tau)$  and  $\Gamma(t, \tau)$  as  $t - \tau \rightarrow 0^+$  and that of  $I(t)$  as  $t - T \rightarrow 0^+$ , then we can use them to derive the asymptotic behaviour of  $f(t)$  as  $t - T \rightarrow 0^+$  by (30).

**Lemma 1** *Let*

$$g(t, \tau) = h(t, \tau) + \frac{\alpha}{2\sqrt{\pi}} \int_{\tau}^t g(\mu, \tau) \frac{(\sqrt{t-\mu})}{(t-\mu)^{\frac{3}{2}}} e^{-\frac{\alpha^2(\sqrt{t-\mu})^2}{4(t-\tau)}} d\mu. \tag{34}$$

If 
$$h(t, \tau) \sim \frac{C_{-\frac{1}{2}}}{(t-\tau)^{\frac{1}{2}}} + C_0 + O((t-\tau)^{\frac{1}{2}}), \text{ as } t-\tau \rightarrow 0^+, \tag{35}$$

then 
$$g(t, \tau) \sim \frac{C_{-\frac{1}{2}}}{(t-\tau)^{\frac{1}{2}}} + C_0 + C_{-\frac{1}{2}} \frac{\alpha\sqrt{\pi}}{4\sqrt{\tau}} + O((t-\tau)^{\frac{1}{2}}), \text{ as } t-\tau \rightarrow 0^+. \tag{36}$$

**Proof** Equation (34) suggests an iteration formula

$$g_{n+1}(t, \tau) = h(t, \tau) + \frac{\alpha}{2\sqrt{\pi}} \int_{\tau}^t g_n(\mu, \tau) \frac{(\sqrt{t-\mu})}{(t-\mu)^{\frac{3}{2}}} e^{-\frac{\alpha^2(\sqrt{t-\mu})^2}{4(t-\tau)}} d\mu, \quad (n \geq 0; g_0(t, \tau) \equiv 0). \tag{37}$$

From (35) we have

$$g_1(t, \tau) = h(t, \tau) \sim \frac{C_{-\frac{1}{2}}}{(t-\tau)^{\frac{1}{2}}} + C_0 + O((t-\tau)^{\frac{1}{2}}), \text{ as } t-\tau \rightarrow 0^+.$$

Then

$$\begin{aligned} g_2(t, \tau) &\sim \frac{C_{-\frac{1}{2}}}{(t-\tau)^{\frac{1}{2}}} + C_0 + O((t-\tau)^{\frac{1}{2}}) \\ &\quad + \frac{\alpha C_{-\frac{1}{2}}}{2\sqrt{\pi}} \int_{\tau}^t \frac{(\sqrt{t-\mu})}{(\mu-\tau)^{\frac{1}{2}}(t-\mu)^{\frac{3}{2}}} e^{-\frac{\alpha^2(\sqrt{t-\mu})^2}{4(t-\tau)}} d\mu \\ &\quad + \frac{\alpha C_0}{2\sqrt{\pi}} \int_{\tau}^t \frac{(\sqrt{t-\mu})}{(t-\mu)^{\frac{3}{2}}} e^{-\frac{\alpha^2(\sqrt{t-\mu})^2}{4(t-\tau)}} d\mu \\ &\quad + O\left(\int_{\tau}^t \frac{(\mu-\tau)^{\frac{1}{2}}(\sqrt{t-\mu})}{(t-\mu)^{\frac{3}{2}}} e^{-\frac{\alpha^2(\sqrt{t-\mu})^2}{4(t-\tau)}} d\mu\right), \text{ as } t-\tau \rightarrow 0^+. \end{aligned}$$

Now

$$\begin{aligned} \int_{\tau}^t \frac{(\sqrt{t-\mu})}{(\mu-\tau)^{\frac{1}{2}}(t-\mu)^{\frac{3}{2}}} e^{-\frac{\alpha^2(\sqrt{t-\mu})^2}{4(t-\tau)}} d\mu &\sim \frac{\pi}{2\sqrt{\tau}} + O((t-\tau)), \text{ as } t-\tau \rightarrow 0^+, \\ \int_{\tau}^t \frac{(\sqrt{t-\mu})}{(t-\mu)^{\frac{3}{2}}} e^{-\frac{\alpha^2(\sqrt{t-\mu})^2}{4(t-\tau)}} d\mu &\sim \frac{(t-\tau)^{\frac{1}{2}}}{\sqrt{t}}, \text{ as } t-\tau \rightarrow 0^+, \\ \int_{\tau}^t \frac{(\mu-\tau)^{\frac{1}{2}}(\sqrt{t-\mu})}{(t-\mu)^{\frac{3}{2}}} e^{-\frac{\alpha^2(\sqrt{t-\mu})^2}{4(t-\tau)}} d\mu &\sim \frac{\pi(t-\tau)}{\sqrt{t}}, \text{ as } t-\tau \rightarrow 0^+. \end{aligned}$$

These expansions imply that

$$g_2(t, \tau) \sim \frac{C_{-\frac{1}{2}}}{\sqrt{(t-\tau)}} + C_0 + \frac{\alpha\sqrt{\pi}C_{-\frac{1}{2}}}{4\sqrt{\tau}} + O((t-\tau)^{\frac{1}{2}}), \text{ as } t-\tau \rightarrow 0^+. \tag{38}$$

From (37) and (38) we have

$$g_3(t, \tau) \sim \text{RHS of (38)}, \text{ as } t-\tau \rightarrow 0^+.$$

Then  $g_n(t, \tau) \sim \text{RHS of (38)}, \quad t - \tau \rightarrow 0^+ (n \geq 2).$

Therefore  $g(t, \tau) \sim \text{RHS of (38)}, \quad t - \tau \rightarrow 0^+. \quad \square$

**Lemma 2** Let  $P(t, \tau)$  be defined by (31). Then it satisfies

$$P(t, \tau) \sim \frac{\alpha}{2k \sqrt{(\pi\tau)} \sqrt{(t-\tau)}} - \frac{\alpha^2}{8k\tau} + O((t-\tau)^{\frac{1}{2}}), \quad \text{as } t - \tau \rightarrow 0^+. \quad (39)$$

**Proof** Let

$$\begin{aligned} J(t, \tau) &= \int_{\alpha\sqrt{\tau}}^{\infty} (\alpha \sqrt{t-\xi}) e^{-i\frac{\alpha\sqrt{t-\xi}}{4(t-\tau)} + \frac{\xi}{4}} d\xi \\ &= \int_{\alpha\sqrt{\tau}}^{\infty} \psi(\xi) e^{g(\xi)/\epsilon} d\xi \end{aligned}$$

where  $\epsilon = t - \tau$ , and

$$\begin{aligned} \psi(\xi) &= (\alpha \sqrt{t-\xi}) e^{-\xi^2/4\epsilon}, \\ \varphi(\xi) &= -\frac{(\alpha \sqrt{t-\xi})^2}{4}. \end{aligned}$$

(i)  $\alpha < 0$ .

Since  $\varphi'(\xi) = \frac{1}{2}(\alpha \sqrt{t-\xi}) < 0$  for  $\xi \in [\alpha \sqrt{\tau}, \infty)$ , it follows that

$$\varphi(\alpha \sqrt{\tau}) = \max \{ \varphi(\xi) \mid \xi \in [\alpha \sqrt{\tau}, \infty) \}.$$

By Laplace's method [12], only the immediate neighbourhood of  $\xi = \alpha \sqrt{\tau}$  contributes to the full asymptotic expansion of the integral  $J(t, \tau)$ . Let

$$B = \alpha(\sqrt{t} - \sqrt{\tau}) \sim \frac{\alpha\epsilon}{2\sqrt{\tau}}, \quad \text{as } \epsilon \rightarrow 0^+. \quad (40)$$

Then

$$\begin{aligned} J(t, \tau) &\sim \int_{\alpha\sqrt{\tau}}^{\alpha\sqrt{\tau}+\delta} \psi(\xi) e^{g(\xi)/\epsilon} d\xi \\ &= \int_0^\delta \psi(\alpha\sqrt{\tau}+s) e^{g(\alpha\sqrt{\tau}+s)/\epsilon} ds \\ &= e^{-\frac{s^2}{4} - \frac{B^2}{\epsilon}} \int_0^\delta \left\{ B + [O(\epsilon) - 1]s + \left[ O(\epsilon) - \frac{(\sqrt{\tau})B - \alpha\epsilon}{2\sqrt{\tau}\epsilon} \right] s^2 + O(s^3) \right\} e^{-\frac{s^2}{4}} ds \\ &\sim -2e^{-\frac{s^2}{4}}(t-\tau) + \frac{\sqrt{(\pi)}\alpha e^{-\frac{s^2}{4}}}{\sqrt{\tau}}(t-\tau)^{\frac{3}{2}} + O((t-\tau)^2), \quad \text{as } t - \tau \rightarrow 0^+. \quad (41) \end{aligned}$$

(ii)  $\alpha > 0$ .

Clearly,

$$J(t, \tau) = \int_0^\infty \psi(\xi) e^{g(\xi)/\epsilon} d\xi - \int_0^{\alpha\sqrt{\tau}} \psi(\xi) e^{g(\xi)/\epsilon} d\xi. \quad (42)$$

Since  $\varphi'(\xi) > 0$  for  $\xi \in [0, \alpha \sqrt{\tau}]$ , it follows that

$$\varphi(\alpha \sqrt{\tau}) = \max \{ \varphi(\xi) \mid \xi \in [0, \alpha \sqrt{\tau}] \}.$$

By Laplace’s method, only the immediate neighbourhood of  $\xi = \alpha \sqrt{\tau}$  contributes to the full asymptotic expansion of the second integral of the RHS of (42). Thus

$$\begin{aligned} \int_0^{\alpha\sqrt{\tau}} \psi(\xi) e^{\sigma(\xi)/\epsilon} \delta\xi &\sim \int_{\alpha\sqrt{(t-\tau)-\delta}}^{\alpha\sqrt{\tau}} \psi(\xi) e^{\sigma(\xi)/\epsilon} d\xi \\ &= \int_0^\delta \psi(\alpha\sqrt{\tau-s}) e^{\sigma(\alpha\sqrt{(t-\tau)-s})/\epsilon} d\xi \\ &\sim 2e^{-\frac{s^2}{4}}(t-\tau) + \frac{\sqrt{\pi}\alpha e^{-\frac{s^2}{4}}}{\sqrt{\tau}}(t-\tau)^{\frac{3}{2}} + O((t-\tau)^2), \text{ as } t-\tau \rightarrow 0^+. \end{aligned} \tag{43}$$

We have

$$\begin{aligned} \int_0^\infty \psi(\xi) e^{\sigma(\xi)/\epsilon} d\xi &= \alpha\sqrt{t} \int_0^\infty \psi(\alpha\sqrt{(t)s}) e^{\sigma(\alpha\sqrt{(t)s})/\epsilon} ds \\ &\sim \alpha\sqrt{t} \int_{1-\delta}^{1+\delta} \psi(\alpha\sqrt{(t)s}) e^{\sigma(\alpha\sqrt{(t)s})/\epsilon} ds \\ &\sim \frac{\alpha^4 t^2}{2\tau} e^{-\frac{s^2}{4t}} \int_{-\infty}^\infty x^2 e^{-\frac{s^2}{4t}x^2} dx + O\left(\int_{-\infty}^\infty x^4 e^{-\frac{s^2}{4t}x^2} dx\right) \\ &= \frac{2a\sqrt{\pi}\alpha e^{-\frac{s^2}{4}}}{\sqrt{\tau}}(t-\tau)^{\frac{3}{2}} + O((t-\tau)^{\frac{5}{2}}), \text{ as } t-\tau \rightarrow 0^+. \end{aligned} \tag{44}$$

From (42), (43) and (44) we get

$$J(t, \tau) \sim -2e^{-\frac{s^2}{4}}(t-\tau) + \frac{\sqrt{\pi}\alpha e^{-\frac{s^2}{4}}}{\sqrt{\tau}}(t-\tau)^{\frac{3}{2}} + O((t-\tau)^2), \text{ as } t-\tau \rightarrow 0^+. \tag{45}$$

From (41) and (45) we have

$$\text{1st term of RHS of (31)} \sim \frac{\alpha}{2k\sqrt{\pi}\sqrt{\tau}(t-\tau)^{\frac{1}{2}}} - \frac{\alpha^2}{4k\tau} + O((t-\tau)^{\frac{1}{2}}), \text{ as } t-\tau \rightarrow 0^+. \tag{46}$$

By (31), (46) and Lemma 1, we have

$$P(t, \tau) \sim \frac{\alpha}{2k\sqrt{\pi}\sqrt{\tau}(t-\tau)^{\frac{1}{2}}} - \frac{\alpha^2}{8k\tau} + O((t-\tau)^{\frac{1}{2}}), \text{ as } t-\tau \rightarrow 0^+. \quad \square$$

**Lemma 3** Let  $\Gamma(t, \tau)$  be defined by (32). Then it satisfies

$$\Gamma(t, \tau) \sim -\frac{\gamma l^2}{2\sqrt{\pi}(t-\tau)^{\frac{1}{2}}} - \frac{\alpha\gamma l^2}{8\sqrt{\tau}} + O((t-\tau)^{\frac{1}{2}}), \text{ as } t-\tau \rightarrow 0^+. \tag{47}$$

**Proof** Considering the first term on the RHS of (32), we have

$$\begin{aligned} \frac{\gamma l^2}{4\sqrt{\pi}(t-\tau)^{\frac{1}{2}}} \int_{\alpha\sqrt{\tau}}^\infty (\alpha\sqrt{(t)-\xi}) e^{-\frac{\gamma(\alpha\sqrt{(t)-\xi})^2}{4(t-\tau)}} d\xi &= -\frac{\gamma l^2}{2\sqrt{\pi}(t-\tau)^{\frac{1}{2}}} e^{-\frac{\gamma(\alpha\sqrt{(t)-\alpha\sqrt{\tau}})^2}{4(t-\tau)}} \\ &= -\frac{\gamma l^2}{2\sqrt{\pi}(t-\tau)^{\frac{1}{2}}} + O((t-\tau)^{\frac{1}{2}}), \text{ as } t-\tau \rightarrow 0^+. \end{aligned} \tag{48}$$



From (32), (48) and Lemma 1, we get

$$\Gamma(t, \tau) \sim -\frac{\gamma l^2}{2\sqrt{(\pi)(t-\tau)^{\frac{3}{2}}}} - \frac{\alpha \gamma l^2}{8\sqrt{\tau}} + O((t-\tau)^{\frac{1}{2}}), \quad t-\tau \rightarrow 0^+. \quad \square$$

**Lemma 4** Let  $I(t)$  be defined by (33). Assume either (1)  $\chi(x) \equiv 0$ ; or (2) for some  $m \geq 0$ ,  $\chi \in C^m[b, \infty)$ ,  $\chi^{(m)}(b) \neq 0$ ,  $\chi^{(i)}(b) = 0$  ( $i = 0, 1, \dots, m-1$ ; for  $m \geq 1$ ), here  $b > \alpha \sqrt{T}$  such that  $\chi(x) = 0$  for  $x \in [\alpha \sqrt{T}, b)$ , and  $\chi(x) \rightarrow C$  as  $x \rightarrow +\infty$  (see (28)). Then

$$I(t) \sim o((t-T)^{-\frac{1}{2}} e^{-\frac{A^2}{t-T}}), \quad \text{as } t-T \rightarrow 0^+, \quad (49)$$

where  $A = (\alpha \sqrt{(T)-b})/2$ .

**Proof** (1)  $\chi(x) \equiv 0$ . In this case equation (33) reduces to a homogeneous Volterra integral equation of the second kind, which has a unique continuous solution

$$I(t) \equiv 0. \quad (50)$$

(2)  $\chi(x)$  not  $\equiv 0$ .

Equation (33) suggests

$$I_{n+1}(t) = -\frac{1}{2\sqrt{(\pi)(t-T)^{\frac{3}{2}}}} \int_{\alpha\sqrt{T}}^{\infty} \chi(\xi) (\alpha\sqrt{(t)-\xi}) e^{-\frac{(\alpha\sqrt{(t)-\xi})^2}{4(t-\tau)}} d\xi + \frac{\alpha}{2\sqrt{\pi}} \int_T^t I_n(\tau) \frac{(\sqrt{t}-\sqrt{\tau})}{(t-\tau)^{\frac{3}{2}}} e^{-\frac{\alpha^2(\sqrt{t}-\sqrt{\tau})}{4(\sqrt{t-\tau})}} d\tau, \quad (n \geq 0; I_0(t) \equiv 0). \quad (51)$$

Case 1.  $m = 0$

$$\begin{aligned} I_1(t) &= -\frac{1}{2\sqrt{(\pi)(t-T)^{\frac{3}{2}}}} \int_b^{\infty} \chi(\xi) (\alpha\sqrt{(t)-\xi}) e^{-\frac{(\alpha\sqrt{(t)-\xi})^2}{4(t-\tau)}} d\xi \\ &\sim -\frac{1}{2\sqrt{(\pi)(t-T)^{\frac{3}{2}}}} \int_b^{\infty} \chi(\xi) (\alpha\sqrt{T-\xi}) e^{-\frac{\alpha^2}{4\sqrt{T}(\alpha\sqrt{T}-\xi)}} \times e^{-\frac{(\alpha\sqrt{(T)-\xi})^2}{4(t-\tau)}} d\xi \\ &\sim \frac{\chi(b)}{\sqrt{(\pi)(t-T)^{\frac{3}{2}}}} e^{-\frac{\alpha^2}{4\sqrt{T}(\alpha\sqrt{T}-b)}} e^{-\frac{(\alpha\sqrt{(T)-b})^2}{4(t-\tau)}} \\ &\sim C_1(t-T)^{-\frac{1}{2}} e^{-\frac{A^2}{t-T}}, \quad b > \alpha \sqrt{T} \quad \text{as } t-T \rightarrow 0^+, \end{aligned}$$

where  $C_1 = \frac{\chi(b)}{\sqrt{\pi}} e^{-(\alpha/4\sqrt{T})(\alpha\sqrt{T}-b)}$ , and  $A = (\alpha \sqrt{(T)-b})/2$ . From (51) we have

$$\begin{aligned} I_2(t) &\sim C_2(t-T)^{-\frac{1}{2}} e^{-\frac{A^2}{t-T}} + \frac{C_2 \alpha}{4\sqrt{(t)A}} (t-T)^{\frac{1}{2}} e^{-\frac{A^2}{t-T}} \\ &\sim C_2(t-T)^{-\frac{1}{2}} e^{-\frac{A^2}{t-T}}, \quad \text{as } t-T \rightarrow 0^+. \end{aligned}$$

Then  $I_n(t) \sim I_1(t)$  as  $t-T \rightarrow 0^+$  ( $n \geq 2$ ), hence

$$I(t) \sim C_2(t-T)^{-\frac{1}{2}} e^{-\frac{A^2}{t-T}}, \quad \text{as } t-T \rightarrow 0^+. \quad (52)$$

Case 2.  $m \geq 1$

Integrating by parts, we can get

$$I_1(t) = \frac{(-1)^{m+1}2^m}{2\sqrt{(\pi)(t-T)^{\frac{3}{2}}}}(t-T) \int_b^\infty F(\alpha\sqrt{t}, \xi) e^{-\frac{(\alpha\sqrt{t}-\xi)^2}{4(t-T)}} d\xi, \tag{53}$$

where

$$F(\alpha\sqrt{t}, \xi) = \underbrace{\frac{d}{d\xi} \left\{ \frac{1}{[\alpha\sqrt{t}-\xi]} \frac{d}{d\xi} \left[ \frac{1}{[\alpha\sqrt{t}-\xi]} \cdots \left[ \frac{1}{[\alpha\sqrt{t}-\xi]} \frac{d\chi(\xi)}{d\xi} \right] \cdots \right\}}_u$$

Let  $\varepsilon = t - T$

$$\begin{aligned} I_1(t) &\sim \frac{(-1)^{m+1}2^{m-1}}{\sqrt{\pi}} e^{m-\frac{3}{2}} \int_b^\infty F(\alpha\sqrt{T}, \xi) e^{-\frac{\xi^2}{4\varepsilon}(\alpha\sqrt{T}-\xi)} e^{-\frac{(\alpha\sqrt{T}-\xi)^2}{4\varepsilon}} d\xi \\ &\sim \frac{(-1)^m 2^m}{\sqrt{(\pi)(\alpha\sqrt{T}-b)}} e^{m-\frac{1}{2}} F(\alpha\sqrt{T}, b) e^{-\frac{\xi^2}{4\varepsilon}(\alpha\sqrt{T}-b)} e^{-\frac{(\alpha\sqrt{T}-b)^2}{4\varepsilon}} \\ &= C_2(t-T)^{m-\frac{1}{2}} e^{-\frac{A^2}{(t-T)}}, \text{ as } t-T \rightarrow 0^+, \end{aligned}$$

where

$$C_2 = (-1)^m \frac{2^m \chi^{(m)}(b)}{\sqrt{(\pi)(\alpha\sqrt{T}-b)^m}} e^{-\frac{\xi^2}{4\varepsilon}(\alpha\sqrt{T}-b)}.$$

In addition,

$$\int_\tau^t (\tau-T)^{m-\frac{1}{2}} \frac{(\sqrt{t}-\sqrt{\tau})}{(t-\tau)^{\frac{3}{2}}} e^{-\frac{\alpha^2(\sqrt{t}-\sqrt{\tau})^2}{4(t-\tau)}} e^{-\frac{A^2}{(t-\tau)}} d\tau \sim C_3(t-T)^m e^{-\frac{A^2}{(t-T)}}, \text{ as } t-T \rightarrow 0^+, \tag{54}$$

where

$$C_3 = \frac{\pi(2m-1)!!}{2^{m+1}m! \sqrt{T}}.$$

From (51) and (54) we get

$$I_2(t) \sim I_1(t), \text{ as } t-T \rightarrow 0^+.$$

So

$$I_n(t) \sim I_1(t), \text{ as } t-T \rightarrow 0^+ (n \geq 2),$$

then

$$I(t) \sim C_2(t-T)^{m-\frac{1}{2}} e^{-\frac{A^2}{(t-T)}}, \text{ as } t-T \rightarrow 0^+. \tag{55}$$

From (50), (52) and (55), we conclude that (49) is true.  $\square$

### 4 Stability analysis

In this section we use the results obtained in the last section to derive the asymptotic behaviour of  $f(t)$  as  $t - T \rightarrow 0^+$ , which we use to examine the linearized stability of the planar solution with respect to non-planar perturbations.

**Theorem 1** *If  $|l| > 0$ ,  $T > 0$ ,  $f \in C^1[T, t]$ ,  $f(T) \neq 0$ , and  $\chi(x)$  satisfy the hypothesis of Lemma 4, then  $f(t)$  has the following asymptotic behaviour:*

$$f(t) \approx f(T) \exp\left(\frac{2l^2}{3\sqrt{\pi}} \left(\frac{\alpha}{\sqrt{T}} - \gamma kt^2\right) (t-T)^{\frac{3}{2}}\right), \text{ for } 0 < t-T \ll 1. \tag{56}$$

**Proof** From (30) and the first terms of (39) and (47), we have

$$\hat{f}(t) \approx kI(t)e^{-t^2} + k(H_1(t) - H_2(t)), \quad 0 < t - T \ll 1, \tag{57}$$

where

$$\begin{aligned} H_i(t) &= \int_T^t F(\tau) G_i(t, \tau) d\tau, \quad (i = 1, 2), \\ F(\tau) &= \hat{f}(\tau) + l^2 f(\tau), \\ G_1(t, \tau) &= D_1 e^{-l^2(t-\tau)} / \sqrt{[\tau(t-\tau)]}, \\ G_2(t, \tau) &= D_2 e^{-l^2(t-\tau)} / \sqrt{(t-\tau)}, \\ D_1 &= \frac{\alpha}{2k\sqrt{\pi}}, \\ D_2 &= \frac{\gamma l^2}{2\sqrt{\pi}}. \end{aligned}$$

Note that  $H_i(t)$  are convergent improper integrals.

Let

$$\begin{aligned} m &= \min \{F(s) \mid T \leq s \leq t\}, \\ M &= \max \{F(s) \mid T \leq s \leq t\}. \end{aligned}$$

Then 
$$m \int_T^t G_i(t, \tau) d\tau \leq H_i(t) \leq M \int_T^t G_i(t, \tau) d\tau, \quad i = 1, 2.$$

Clearly, the  $G_i(t, \tau)$  do not change sign on  $\tau \in (T, t)$ . Without loss of generality, assume  $\int_T^t G_i(t, \tau) d\tau > 0 (i = 1, 2)$ . So

$$m \leq \frac{H_i(t)}{\int_T^t G_i(t, \tau) d\tau} \leq M, \quad i = 1, 2.$$

Define  $\mu_i$  such that

$$H_i(t) = \mu_i \int_T^t G_i(t, \tau) d\tau, \quad i = 1, 2. \tag{58}$$

Since  $F \in C[T, t]$ , by the Intermediate Value Theorem, there exist  $\tau_i^* \in [T, t]$  such that  $F(\tau_i^*) = \mu_i (i = 1, 2)$ . From the assumption  $f(T) \neq 0$ , equation (30) and lemma 4, we can get  $F(t) \neq 0$  when  $0 < t - T \ll 1$ . So  $F(\tau_i^*) - F(t) \ll F(t)$  as  $t - \tau_i^* \rightarrow 0^+$ , i.e.  $F(\tau_i^*) \sim F(t)$  as  $t - \tau_i^* \rightarrow 0^+ (i = 1, 2)$ .

Hence, (58) becomes

$$H_i(t) \approx F(t) \int_T^t G_i(t, \tau) d\tau, \quad i = 1, 2.$$

Furthermore, (57) becomes

$$\hat{f}(t) \approx kI(t)e^{-t^2} + kF(t) \left[ \int_T^t G_1(t, \tau) d\tau - \int_T^t G_2(t, \tau) d\tau \right], \quad 0 < t - T \ll 1. \tag{59}$$

Since 
$$\int_{\tau}^t G_1(t, \tau) d\tau \sim \frac{2D_1}{\sqrt{T}}(t-T)^{\frac{1}{2}}, \text{ as } t-T \rightarrow 0^+$$

and 
$$\int_{\tau}^t G_2(t, \tau) d\tau \sim 2D_2(t-T)^{\frac{1}{2}}, \text{ as } t-T \rightarrow 0^+,$$

(59) becomes

$$f(t) \approx kI(t)e^{-t^2\tau} + 2k[f(t) + I^2 f(t)] \left( \frac{D_1}{\sqrt{T}} - D_2 \right) (t-T)^{\frac{1}{2}}, \quad 0 < t-T \ll 1.$$

Hence

$$\begin{aligned} f(t) &\approx \exp \left( \left[ 2kl^2 \left( \frac{D_1}{\sqrt{T}} - D_2 \right) \int (t-T)^{\frac{1}{2}} dt \right] \right) \\ &\quad \times \left[ \int kI(t) e^{-t^2\tau} e^{-\int 2kt^2 \left( \frac{D_1}{\sqrt{T}} - D_2 \right) (t-T)^{\frac{1}{2}} dt} dt + \text{Const} \right] \\ &\approx \exp \left( \left[ \frac{4}{3}kl^2 \left( \frac{D_1}{\sqrt{T}} - D_2 \right) (t-T)^{\frac{3}{2}} \right] \right) \\ &\quad \times \left[ k e^{-t^2\tau} \int I(t) dt + \text{Const} \right], \quad 0 < t-T \ll 1. \end{aligned} \tag{60}$$

By Lemma 4, we know

$$I(t) = o((t-T)^{-\frac{1}{2}} e^{-\frac{t^2}{t-T}}) = o((t-T)^{-\frac{1}{2}}), \text{ as } t-T \rightarrow 0^+.$$

So 
$$\int I(t) dt = o((t-T)^{\frac{1}{2}}), \text{ as } t-T \rightarrow 0^+. \tag{61}$$

If  $t = T$ , we get  $\text{Const} \approx f(T) \neq 0$ . Thus (60) becomes

$$f(t) \approx f(T) \exp \left( \frac{2l^2}{3\sqrt{\pi}} \left( \frac{\alpha}{\sqrt{T}} - \gamma kl^2 \right) (t-T)^{\frac{3}{2}} \right), \quad 0 < t-T \ll 1. \quad \square$$

Using Theorem 1 we now investigate shape stability in the following physical situations:

(1) Melting problem ( $\alpha < 0$ ).

Since  $\gamma \geq 0, k > 0$ , it follows that

$$\frac{2l^2}{3\sqrt{\pi}} \left( \frac{\alpha}{\sqrt{T}} - \gamma kl^2 \right) < 0.$$

Thus the melting problem is linearly stable regardless of the presence of surface tension effects.

(2) Solidification problem ( $\alpha > 0$ ).

From (56) we see that every mode of the solidification problem is linearly unstable without surface tension ( $\gamma = 0$ ).

The solidification problem with surface tension ( $\gamma > 0$ ) is linearly stable for those modes which satisfy

$$|l| > \sqrt{\left(\frac{\alpha}{\gamma k \sqrt{T}}\right)}. \quad (62)$$

Thus, to get a stable solidification problem with surface tension for a given mode  $l$ , the velocity of the free boundary should satisfy

$$V = \frac{d}{dt} R_p(t)|_{t=\tau} = \frac{\alpha}{2\sqrt{T}} < \frac{k\gamma l^2}{2}. \quad (63)$$

This is precisely the same formula that was obtained by Ockendon [11] using a travelling wave base state in the singular case that  $ku_\infty = 1$ , and that Chadam & Ortoleva [4] obtained when  $T \rightarrow \infty$ , or equivalently,  $\alpha$  and  $V = \alpha/2\sqrt{T} \rightarrow 0$ .

Finally, from (60) and (61) we have shown the following result which says that the onset of shape instabilities arises autonomously through geometric interactions if one eliminates perturbations in the concentration profile near the boundary.

**Theorem 2** Under the hypothesis of Theorem 1, equation (30) is equivalent to

$$\hat{f}(t) = k \int_{\tau}^t [\hat{f}(\tau) + l^2 f(\tau)] e^{-l^2(t-\tau)} [P(t, \tau) + \Gamma(t, \tau)] d\tau \quad (64)$$

in the limit  $t - T \rightarrow 0^+$ , i.e. the effect of the initial data  $\chi(x)$  is subdominant to the term on the right hand side of (56).

(Note that the special solution  $f(t) \equiv 0$  is excluded by the assumption  $f(T) \neq 0$ .)

## 5 Numerical verification

To verify our theoretical results numerically, we have developed a boundary integral numerical technique whose details can be found in a separate paper [13]. Here we only sketch the idea and present the numerical results.

Instead of using (24)–(28) to verify (56), we apply the integro-differential and integral equations (30)–(33). By theorem 2 we know that only (30)–(32) are dominant equations. So if we can verify (39) and (47) numerically from (31) and (32), and verify (56) from (64), then our theoretical results have been verified numerically.

Since there is a singularity at  $t = \tau$  in (39) and (47), we cannot verify (39) and (47) directly. Fortunately, we can remove the singularity by multiplying (39) and (47) by  $(t - \tau)^{\frac{1}{2}}$ . Thus verification of (39) and (47) is reduced to establishing that

$$\begin{aligned} \bar{P}(t, \tau) &= (t - \tau)^{\frac{1}{2}} P(t, \tau) \\ &\sim \frac{\alpha}{2k\sqrt{\pi\tau}} - \frac{\alpha^2}{8k\tau} (t - \tau)^{\frac{1}{2}} + O((t - \tau)^{\frac{3}{2}}), \quad t - \tau \rightarrow 0^+, \end{aligned} \quad (65)$$

and

$$\begin{aligned} \bar{\Gamma}(t, \tau) &= (t - \tau)^{\frac{1}{2}} \Gamma(t, \tau) \\ &\sim -\frac{\gamma l^2}{2\sqrt{\pi}} - \frac{\alpha\gamma l^2}{8\sqrt{\tau}} (t - \tau)^{\frac{1}{2}} + O((t - \tau)^{\frac{3}{2}}), \quad t - \tau \rightarrow 0^+. \end{aligned} \quad (66)$$

Table 1  $T\_MAX = 0.1001$ ,  $X\_MAX = 1.0$ ,  $T\_NUM = 500$ ,  $X\_NUM = 4000$ ,  $T = 0.1$ ,  $k = 0.5$ ,  $S = 0.5$

$t$	num- $\bar{P}(t, T)$	asy- $\bar{P}(t, T)$	(asy-num)/asy
1.0000000e-01	1.54416513e+00	1.54416513e+00	0.0000000e+00
1.0000020e-01	1.54332398e+00	1.54332761e+00	2.35496432e-06
1.0000040e-01	1.54298239e+00	1.54298071e+00	-1.09318866e-06
1.0000060e-01	1.54271934e+00	1.54271451e+00	-3.12864539e-06
1.0000080e-01	1.54249459e+00	1.54249010e+00	-2.91249390e-06
1.0000100e-01	1.54229528e+00	1.54229239e+00	-1.87345205e-06
.....	.....	.....	.....
1.0009920e-01	1.52409614e+00	1.52551279e+00	9.28640216e-04
1.0009940e-01	1.52407447e+00	1.52549400e+00	9.30536252e-04
1.0009960e-01	1.52405282e+00	1.52547523e+00	9.32432274e-04
1.0009980e-01	1.52403119e+00	1.52545647e+00	9.34328283e-04
1.0010000e-01	1.52400958e+00	1.52543773e+00	9.36224279e-04

From (31) and (32) we see that  $\bar{P}(t, \tau)$  and  $\bar{\Gamma}(t, \tau)$  satisfy

$$\begin{aligned} \bar{P}(t, \tau) = 2(t-\tau)^{\frac{1}{2}} \int_{x, \nu, \tau}^{\infty} \frac{\partial u_p}{\partial X}(\xi, \tau) E_x(R_p(t), \xi, t, \tau) d\xi \\ - 2(t-\tau)^{\frac{1}{2}} \int_{\tau}^t \frac{\bar{P}(\mu, \tau)}{(\mu-\tau)^{\frac{1}{2}}} E_x(R_p(t), R_p(\mu), t, \mu) d\mu, \end{aligned} \tag{67}$$

and

$$\begin{aligned} \bar{\Gamma}(t, \tau) = -\gamma t^2(t-\tau)^{\frac{1}{2}} \int_{x, \nu, \tau}^{\infty} E_x(R_p(t), \xi, t, \tau) d\xi \\ - 2(t-\tau)^{\frac{1}{2}} \int_{\tau}^t \frac{\bar{\Gamma}(\mu, \tau)}{(\mu-\tau)^{\frac{1}{2}}} E_x(R_p(t), R_p(\mu), t, \mu) d\mu. \end{aligned} \tag{68}$$

Fixing  $\tau \geq T$ , we discretize (67) and (68) by using Gauss quadrature and the trapezoidal rule. We then get the numerical formulas

$$\begin{aligned} \bar{P}_i(\tau) &= FP(\bar{P}_0, \bar{P}_1, \dots, \bar{P}_{i-1}), \\ \bar{\Gamma}_i(\tau) &= F\Gamma(\bar{\Gamma}_0, \bar{\Gamma}_1, \dots, \bar{\Gamma}_{i-1}) \end{aligned}$$

where  $\bar{P}_i(\tau) = \bar{P}(t_i, \tau)$ ,  $\bar{\Gamma}_i(\tau) = \bar{\Gamma}(t_i, \tau)$ ,  $t_i = \tau + i\Delta t$ ,  $\Delta t \geq 0$ ,  $i \geq 0$ . The concrete expressions of  $FP$  and  $F\Gamma$  are omitted here.

The numerical results and asymptotic results agree well and get closer as  $t - T \rightarrow 0^+$ , which is what is expected because the asymptotic results become more accurate as  $t - T \rightarrow 0^+$ . We give some of the numerical results in Tables 1 and 2 to demonstrate this observation.

We now proceed to verify numerically that equation (64) gives the asymptotic estimate of  $f(t)$  implied in equation (56) for  $0 < t - T \ll 1$ , when the asymptotic estimates of  $P(t, \tau)$  and  $\Gamma(t, \tau)$  given in lemmas 2 and 3 are used. By lemmas 2 and 3 and equation (64), we have

$$f(t) \approx k \int_{\tau}^t [f(\tau) + l^2 f(\tau)] e^{-t^2(u-\tau)} \left[ \frac{D_1}{\sqrt{(\tau)(t-\tau)^{\frac{1}{2}}} - \frac{D_2}{(t-\tau)^{\frac{1}{2}}} \right] d\tau, \quad 0 < t - T \ll 1. \tag{69}$$

Table 2  $T\_MAX = 0.1001$ ,  $T\_NUM = 500$ ,  $T = 0.1$ ,  $l = 0.5$ ,  $r = 0.5$ ,  $S = 0.5$

$t$	$num\_f(t, T)$	$asy\_f(t, T)$	$(asy-num)/asy$
1.0000000e-01	-3.52618490e-02	-3.52618490e-02	0.0000000e+00
1.0000020e-01	-3.52811274e-02	-3.52809741e-02	-4.34618825e-06
1.0000040e-01	-3.52891161e-02	-3.52888959e-02	-6.23897475e-06
1.0000060e-01	-3.52953141e-02	-3.52949746e-02	-9.61879969e-06
1.0000080e-01	-3.53004936e-02	-3.53000992e-02	-1.11723135e-05
1.0000100e-01	-3.53050385e-02	-3.53046140e-02	-1.20253274e-05
.....	.....	.....	.....
1.0009920e-01	-3.56897537e-02	-3.56877852e-02	-5.51590920e-05
1.0009940e-01	-3.56901856e-02	-3.56882143e-02	-5.52376423e-05
1.0009960e-01	-3.56906172e-02	-3.56886430e-02	-5.53161773e-05
1.0009980e-01	-3.56910483e-02	-3.56890713e-02	-5.53946970e-05
1.0010000e-01	-3.56914790e-02	-3.56894992e-02	-5.54732012e-05

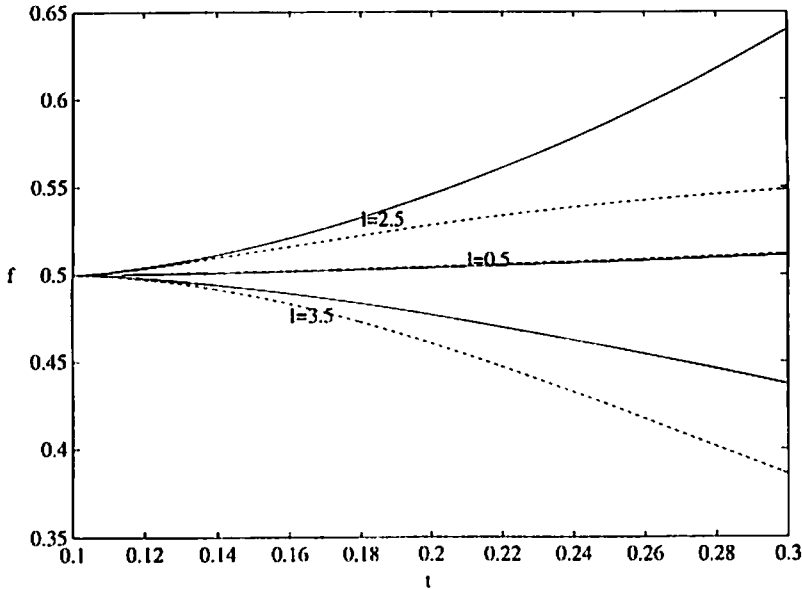


FIGURE 1. Solidification problem with surface tension.  $\alpha = 0.865503 > 0$ ; RHS of (62) = 3.308753; — = asymptotic solution; --- = numerical solution.  $k = s = r = 0.5$ ,  $T = 0.1$ ,  $f(T) = 0.5$ .

Discretizing equation (69) using the trapezoidal rule and using asymptotic analysis, we obtain

$$f^m = FF(f^0, f^1, \dots, f^{m-1}) \tag{70}$$

where  $f^m = f(t_m)$ ,  $t_m = T + m \Delta t$ ,  $\Delta t > 0$ ,  $m \geq 0$ . The expression of  $FF$  is omitted here.

We use the asymptotic solution (56) and numerical formula (70) to obtain figures 1–3. Figure 1 demonstrates that the solidification problem with surface tension is linearly stable for modes satisfying the relation (62) since the corresponding curve is decreasing for  $t$  near

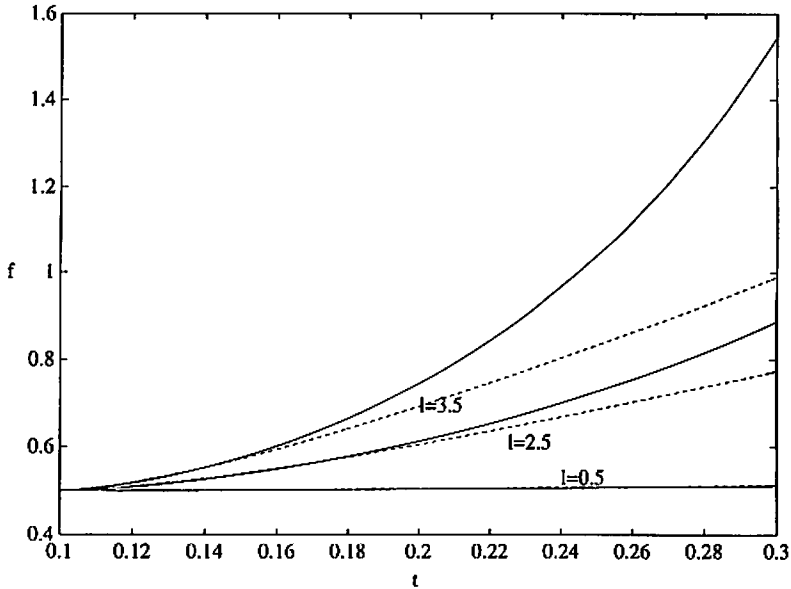


FIGURE 2. Solidification problem without surface tension.  $\alpha = 0.865503 > 0$ ; — = asymptotic solution; --- = numerical solution.  $k = s = 0.5$ ,  $r = 0.0$ ,  $T = 0.1$ ,  $f(T) = 0.5$ .

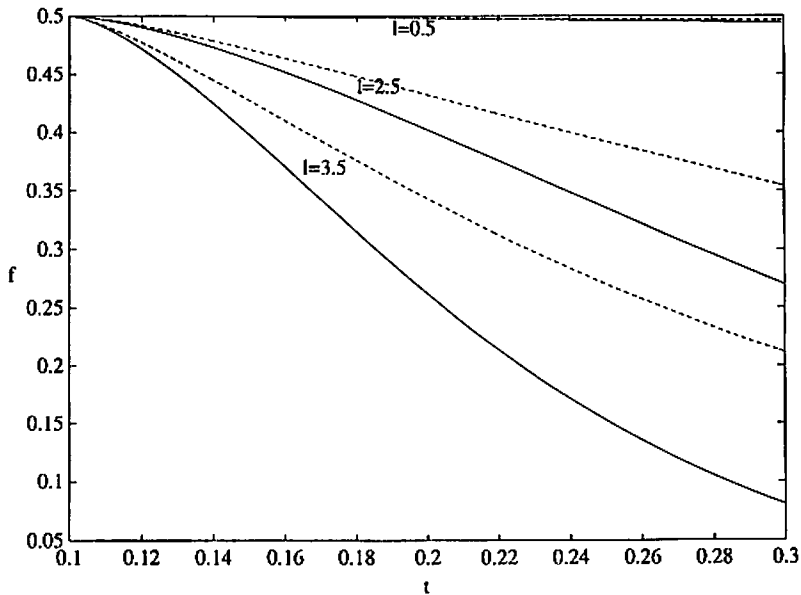


FIGURE 3. Melting problem.  $\alpha = 0.865503 > 0$ ; — = asymptotic solution; --- = numerical solution.  $k = s = 0.5$ ,  $r = 0.0$ ,  $T = 0.1$ ,  $f(T) = 0.5$ .

the initial time  $T$ , and is linearly unstable for those modes not satisfying (62), since the corresponding curve is increasing for  $t$  near  $T$ . Figure 2 verifies that every mode of the solidification problem is linearly unstable without surface tension since all the curves are increasing for  $t$  near  $T$ . Figure 3 demonstrates that the melting problem is always linearly



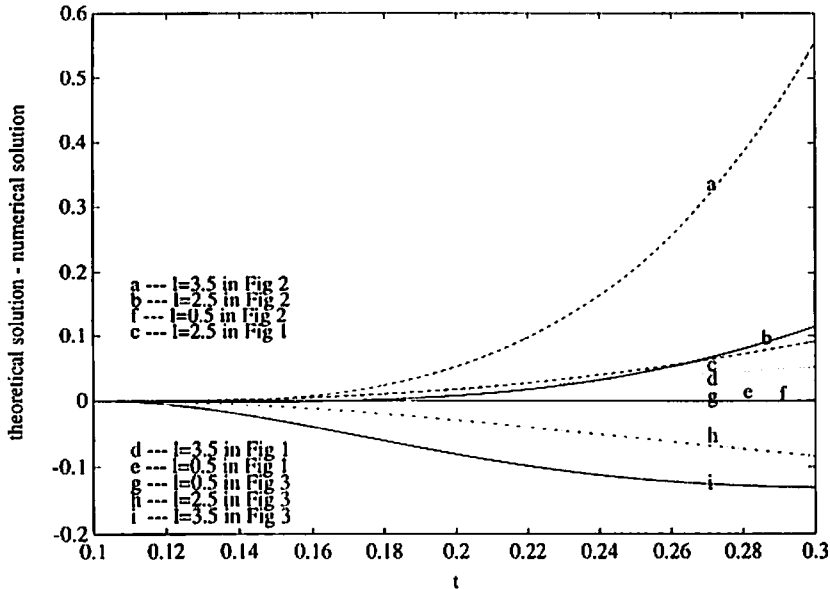


FIGURE 4. Errors for figures 1-3.

stable. Figure 4 demonstrates that the asymptotic solution (56) and numerical solution given by (70) agree with each other well when  $t - T$  is very small.

## 6 Summary

The linearized shape stability of the planar solution of a time dependent version of Mullins & Sekerka's [1] model with respect to non-planar perturbations has been discussed. The linearized asymptotic stability was given in [4], i.e. for  $T \rightarrow \infty$ , or equivalently, for fronts with velocity  $\alpha/2 \sqrt{T} \rightarrow 0$ . Here we examine the linearized stability for  $T < \infty$ , i.e. for fronts with arbitrary velocities.

Using asymptotic analysis, the linearized integral equation for the amplitude of the shape perturbation is used to find a stability condition involving the parameters of the problem. Specifically, the  $e^{i\theta}$  mode is stable if

$$|l| > \sqrt{\left(\frac{\alpha}{\gamma k \sqrt{T}}\right)} = \sqrt{\left(\frac{2V}{\gamma k}\right)},$$

which is precisely Chadam & Ortoleva's [4] result derived for  $T \rightarrow \infty$  (i.e.  $\alpha \rightarrow 0$ ) and that of Ockendon [11] derived in the singular case  $ku_\infty = 1$  using travelling waves as base planar states.

We have also shown that the effect of the initial data in studying the linearized shape stability of the problem is subdominant provided that the perturbation of the concentration field in the vicinity of the front can be neglected.

By using the trapezoidal rule, Gauss quadrature and asymptotic analysis, we develop a numerical scheme to compute the amplitude of the perturbation,  $f(t)$ , defined by (30) for

$t$  near  $T$ . Our numerical and theoretical results agree for  $t$  near the initial time  $T$  – the region for which they were designed.

### References

- [1] MULLINS, W. W. & SEKERKA, J. 1963 Morphological stability of a particle growing by diffusion or heat flow. *J. Appl. Phys.* **34**, 323–329.
- [2] LANGER, J. S. 1980 Instabilities and pattern formation in crystal growth. *Rev. Mod. Phys.* **52**, 1–28.
- [3] TURLAND, B. D. & PECKOVER, R. S. 1980 The stability of planar melting fronts in two-phase thermal Stefan problems. *IMA J. Appl. Math.* **25**, 1–5.
- [4] CHADAM, J. & ORTOLEVA, P. 1983 The stabilizing effect of surface tension on the development of the free boundary in a planar, one-dimensional, Cauchy–Stefan problem. *IMA J. Appl. Math.* **30**, 57–66.
- [5] CHADAM, J., BAILLON, J. C., BERTSCH, M., ORTOLEVA, P. & PELETIER, L. 1984 *College de France Seminar, Vol. VI* (Brezis, H. and Lions, J. L. (Eds)). *Research Notes in Mathematics* **109**, 27–47, Pitman.
- [6] RICCI, R. & XIE, W. 1991 On the stability of some solutions of the Stefan problem. *Euro. J. Appl. Math.* **2**, 1–15.
- [7] DEWYNNE, N., HOWISON, S. D., OCKENDON, J. R. & XIE, W. 1989 Asymptotic behaviour of solutions to the Stefan problem with a kinetic condition at free boundary. *J. Austral. Math. Soc., Ser. B*, **31**, 81–96.
- [8] MAHLER, E. G., SCHECHTER, R. S. & WISSLER, E. H. 1968 Stability of a fluid layer with time-dependent density gradients. *Phys. Fluids* **11**, 1901–1912.
- [9] CARSLAW, H. S. & JAEGER, J. C. 1959 *Conduction of Heat in Solids*. Clarendon, Oxford.
- [10] RUBINSTEIN, L. 1982 Global stability of the Neumann solution of two-phase Stefan problems. *IMA J. Appl. Math.* **28**.
- [11] OCKENDON, J. 1979 Linear and non-linear stability of a class of moving boundary problems. In: *Proc. Seminar on Free Boundary Problems*, Pavia, Italy.
- [12] BENDER, C. M. & ORSZAG, S. A. 1978 *Advanced Mathematical Methods for Scientists and Engineers*. McGraw-Hill.
- [13] ZHU, Q., PEIRCE, A. & CHADAM, J. A boundary integral numerical technique for free boundary problems (in preparation).